The American Journal of Human Genetics, Volume *99*

Supplemental Data

Biallelic Mutations in *MITF* Cause Coloboma, Osteopetrosis, Microphthalmia, Macrocephaly, Albinism, and Deafness

Aman George, Dina J. Zand, Robert B. Hufnagel, Ruchi Sharma, Yuri V. Sergeev, Janet M. Legare, Gregory M. Rice, Jessica A. Scott Schwoerer, Mariana Rius, Laura Tetri, David M. Gamm, Kapil Bharti, and Brian P. Brooks

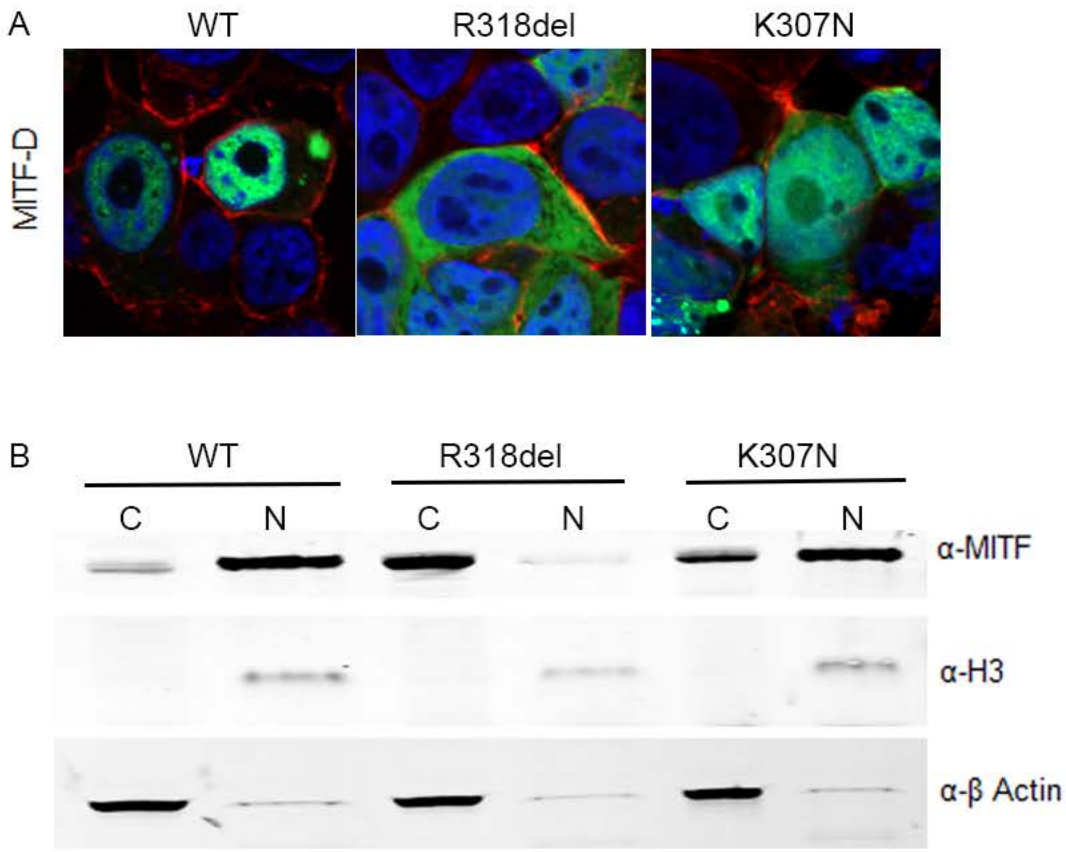
A
WT
R318del
K307N
MITF-D
B
WT
R318del
K307N
C
N
C
N
C
N
α-MITF
α-H3
α-β Actin

Figure S1. Subcellular localization of WT and mutant MITF-D protein.

(A) Green fluorescent protein (GFP) tagged WT-MITF-D isoform was observed predominantly in the nucleus of transfected HEK293 cells. The R318del protein was observed only in the cytoplasm and not in the nucleus, whereas the K307N mutant localized both in the cytoplasm and the nucleus, suggesting some disruption of the nuclear migration ability (also see Supplementary movie). For live cell imaging approximately 1×10^4/well HEK293T cells were cultured in a 4-well glass bottom chamber slide for 24 hrs, and then transiently transfected with fluorescent protein tagged WT and/or mutant MITF constructs. After 24 hrs of transfection, cells were washed three times with cell culture medium and imaged for 15-16 hrs in standard cell culture medium at 37°C and 5% CO2. Every 6 mins, 11 or 13 z-stacks at 20X magnification were acquired in GFP, RFP and DIC channels for each WT and mutant transfection combination using a Zeiss 780 confocal microscope. Time lapse movies were exported from maximum intensity projected Z-image series for each transfection group. The images were analyzed using ZEN Software (Carl Zeiss Microscopy LLC, Thornwood, NY, USA). The experiment was repeated three times for each MITF-A and D. (B) The subcellular localization of mutants was further confirmed by Western blot analysis of the cytoplasmic “C” and nuclear “N” fractions of HEK293 cells transfected by WT and mutant MITF-D isoform, and was observed to be in agreement with the fluorescence microscopy data.

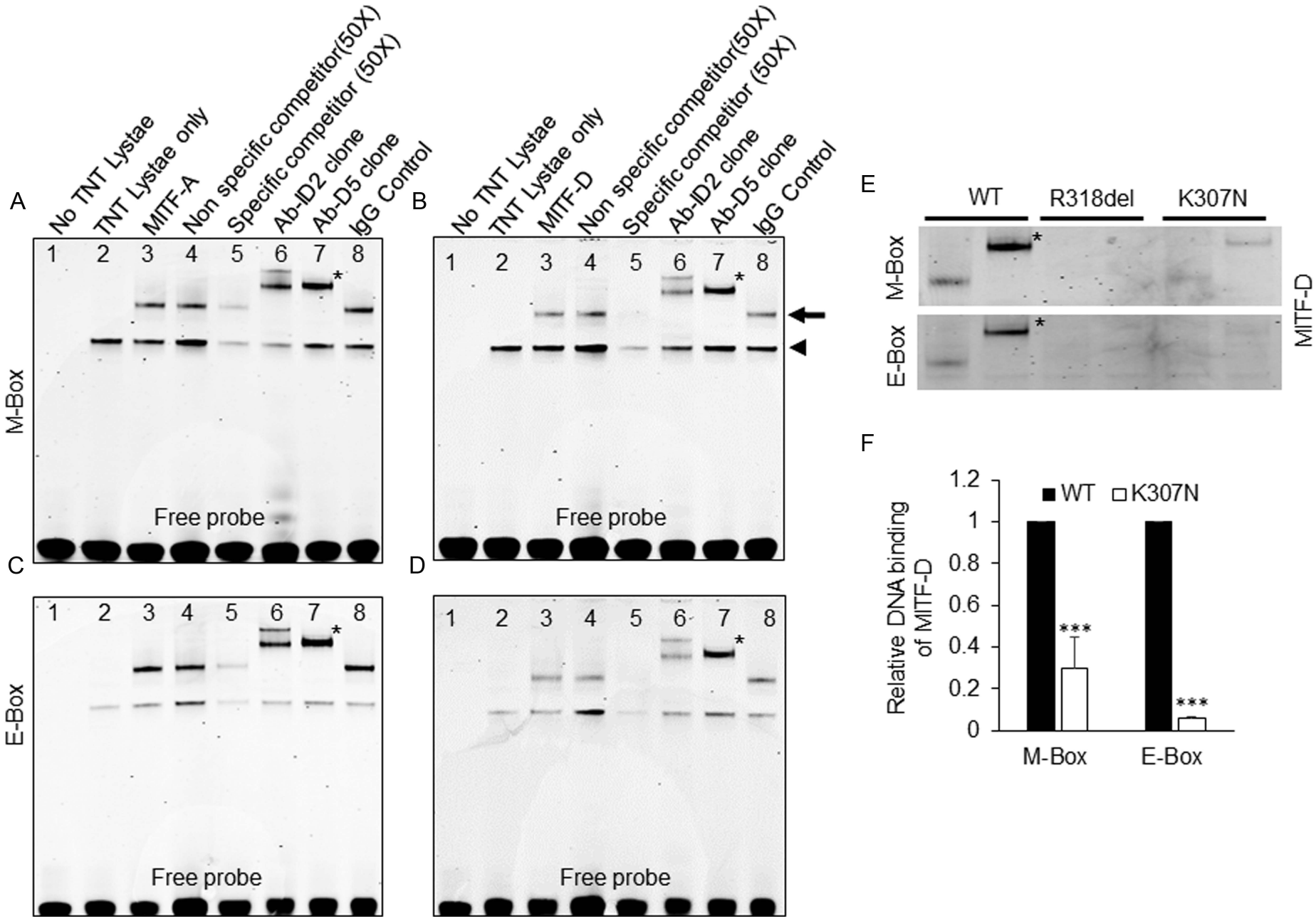
A
No TNT Lystae
TNT Lystae only
MITF-A
Non specific competitor(50X)
Specific competitor (50X)
Ab-ID2 clone
Ab-D5 clone
IgG Control
1 2 3 4 5 6 7 8
M-Box
Free probe
B
No TNT Lystae
TNT Lystae only
MITF-D
Non specific competitor(50X)
Specific competitor (50X)
Ab-ID2 clone
Ab-D5 clone
IgG Control
1 2 3 4 5 6 7 8
Free probe
C
1 2 3 4 5 6 7 8
E-Box
Free probe
D
1 2 3 4 5 6 7 8
Free probe
E
WT
R318del
K307N
M-Box
E-Box
MITF-D
F
Relative DNA binding of MITF-D
WT
K307N
1.2
1
0.8
0.6
0.4
0.2
0
***
***
M-Box
E-Box

Figure S2. Electrophorectic mobility shift assay (EMSA) of WT and mutant MITF (A- and D-isoforms).

(A, B, C and D) EMSAs with *in vitro* translated (IVT) wild type MITF-A and MITF-D proteins incubated with IR-700 labelled probes containing M-Box and E-Box sequences. TnT® reticulocyte lysate alone resulted in a non-specific, shifted band (lane 2, arrowhead) of probe (lane 1), distinct from that observed with IVT MITF protein (lane 3, arrow). Unlabeled nonspecific probe (oligonucleotide with mutated M-Box and E-Box binding site, 50x input, lane 4) did not alter the binding signal, but unlabeled probe (unlabeled oligonucleotide with consensus M-Box and E-Box sequence, 50x input, lane 5), did. Two different anti-MITF antibody clones (ID2 and D5) could supershift (*) the MITF binding signal (lanes 6 & 7, respectively). Supershift was not observed with an IgG control antibody (lane 8). (E and F) The DNA binding ability of MITF-D K307N mutant to the M-Box and E-Box sequence was significantly reduced as compared to the WT-MITF. The R318del mutant did not bind M-Box or E-Box sequences as previously reported. In cases where the DNA binding effect of WT protein + mutant protein was studied, the two proteins were co-transcribed and co-translated, unlike previous report where the proteins are synthesized separately and then mixed later.[1] (F) The graph provides the quantification of the DNA binding by the MITF-D wild type and K307N mutant protein to oligonucleotides carrying consensus M-Box and E-Box elements, as calculated from three different trials. In all comparisons, *P* values were calculated using the Student's *t* test (one sided distribution). ***P<0.005

A

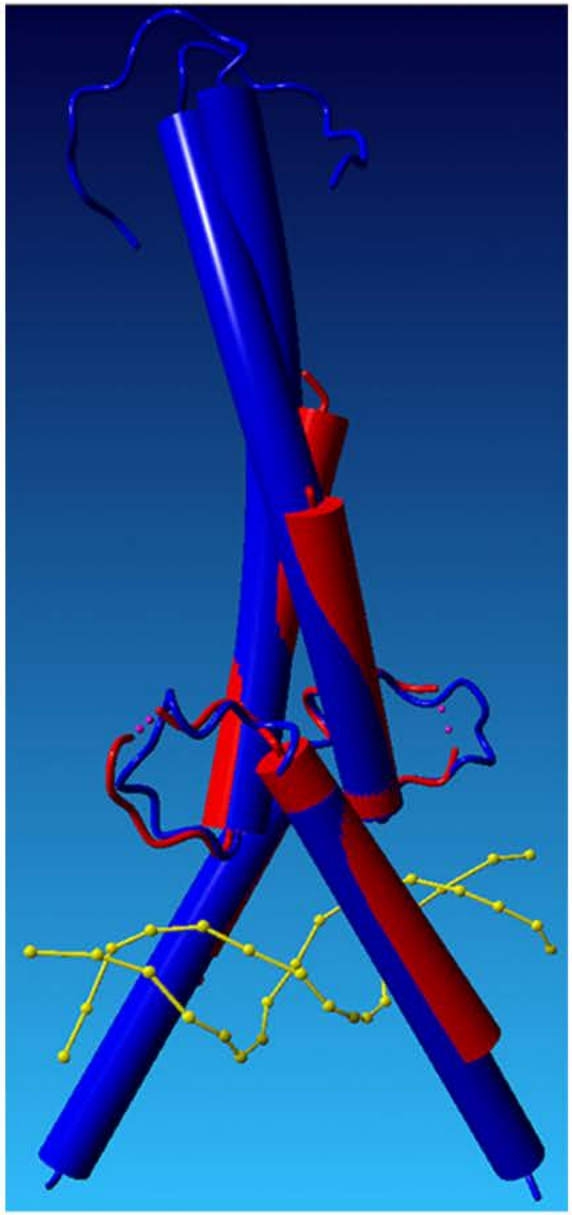

B

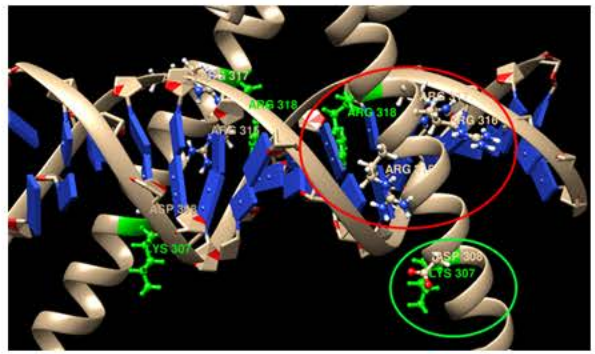
ARG 318
ARG 318
ARG 310
LYS 307
ASP 306
LYS 307

C

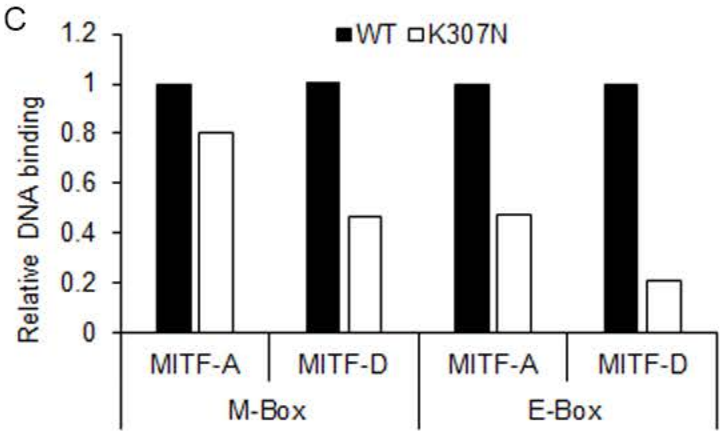
WT
K307N
Relative DNA binding
1.2
1
0.8
0.6
0.4
0.2
0
MITF-A
MITF-D
MITF-A
MITF-D
M-Box
E-Box

D

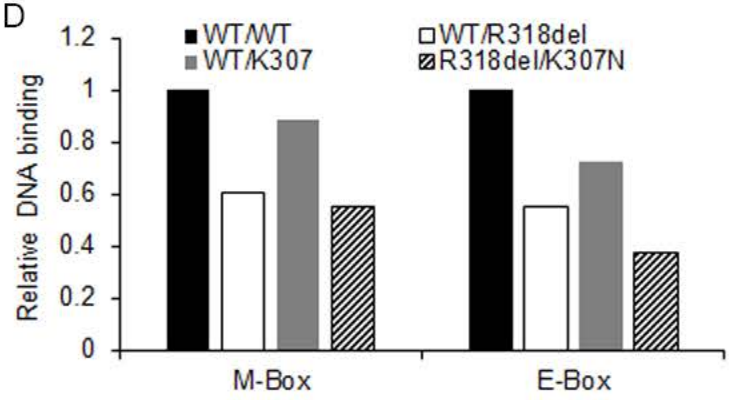
WT/WT
WT/K307
WT/R318del
R318del/K307N
Relative DNA binding
1.2
1
0.8
0.6
0.4
0.2
0
M-Box
E-Box

Figure S3. Molecular modeling of DNA/MITF complexes for four family 1 members

The amino acid sequences of A- and D-isoforms of MITF were retrieved from the UniProtKB database (http://www.uniprot.org/uniprot/O75030). The structures of MITF-DNA homo- and hetero-complexes were generated using molecular visualization, modeling, and dynamics program Yasara[2] (http://www.yasara.org/) and structural templates such as the MITF apo structure (PDB file: 4ATH), MITF: M-box complex (PDB file: 4ATI), and MITF: E-box complex (PDB file: 4ATK). Two wild type complexes and eight mutant variants associated with either the MITF A-isoform or the D-isoform were built as MITF:M-Box or MITF:E-Box homo-dimers. In addition, 16 protein hetero-complexes were built to mimic M-box/E-box complexes formed by the MITF A-isoform: WT/R318del (father), WT/K307N (mother), K307N/R318del (son), WT/WT (daughter); or the MITF D-isoform. All 26 homo- and hetero-complexes were refined, 1 ns equilibrated at 37°C using a 149.4 Å x 89.6 Å x 61.5 Å water box using Amber 99 force field. Finally, binding energy was calculated in aqueous medium as the energy at indefinite distance (between DNA and the rest of the complex) minus the complex energy in the bound state. Molecular visualization was also performed by using the UCSF Chimera (http://www.cgl.ucsf.edu/chimera/). (A) The structure of wild type MITF-A isoform bound to the consensus E-box DNA sequence was prepared by molecular modeling (represented in blue) using the already available crystallographic structure of MITF-M as a template (shown in red). The two structures were then merged to represent the fitness of the modelling. Other complexes comprising of mutant MITF-A isoforms, and wild type and mutant MITF-D isoforms bound to the DNA were built (data not shown), as described in methods section. (B) The Needleman-Wunsch structural alignment shows a loose structural fitting of the deletion mutant to the crystallographic template (root mean square of 3.2 Å), compared to that of a wild type or the variant with missense mutation

in both MITF-A and –D isoforms (r.m.s. of 0.9-1.5 Å). This observation suggests that deletion in position 318 causes a more significant change in the subunit structure than that of the K307N mutant. (C) Initial comparison of WT and mutant MITF protein models predicts a trend of decreasing DNA binding of homodimers to the DNA in the following order: wt/wt>K307N/K307N>R318del/R318del. Moreover the 15 ns equilibration of the deletion mutant complex shows complex dissociation and complete loss of DNA binding (data not shown). This suggests that deletion variants do not favor a DNA binding complex and agree with the observation that R318del variant does not bind DNA (therefore not shown in the graph C). (D) In case of the WT/mutant combination, three different complexes i.e. WT+WT, WT+mutant and mutant+mutant, are possible. The binding energy, for each of these complexes was determined using molecular modelling since it could not have been done experimentally. The observed binding energies were then combined for all of the patient genotypes and were consistent with the EMSA data (Figure 3C graph).

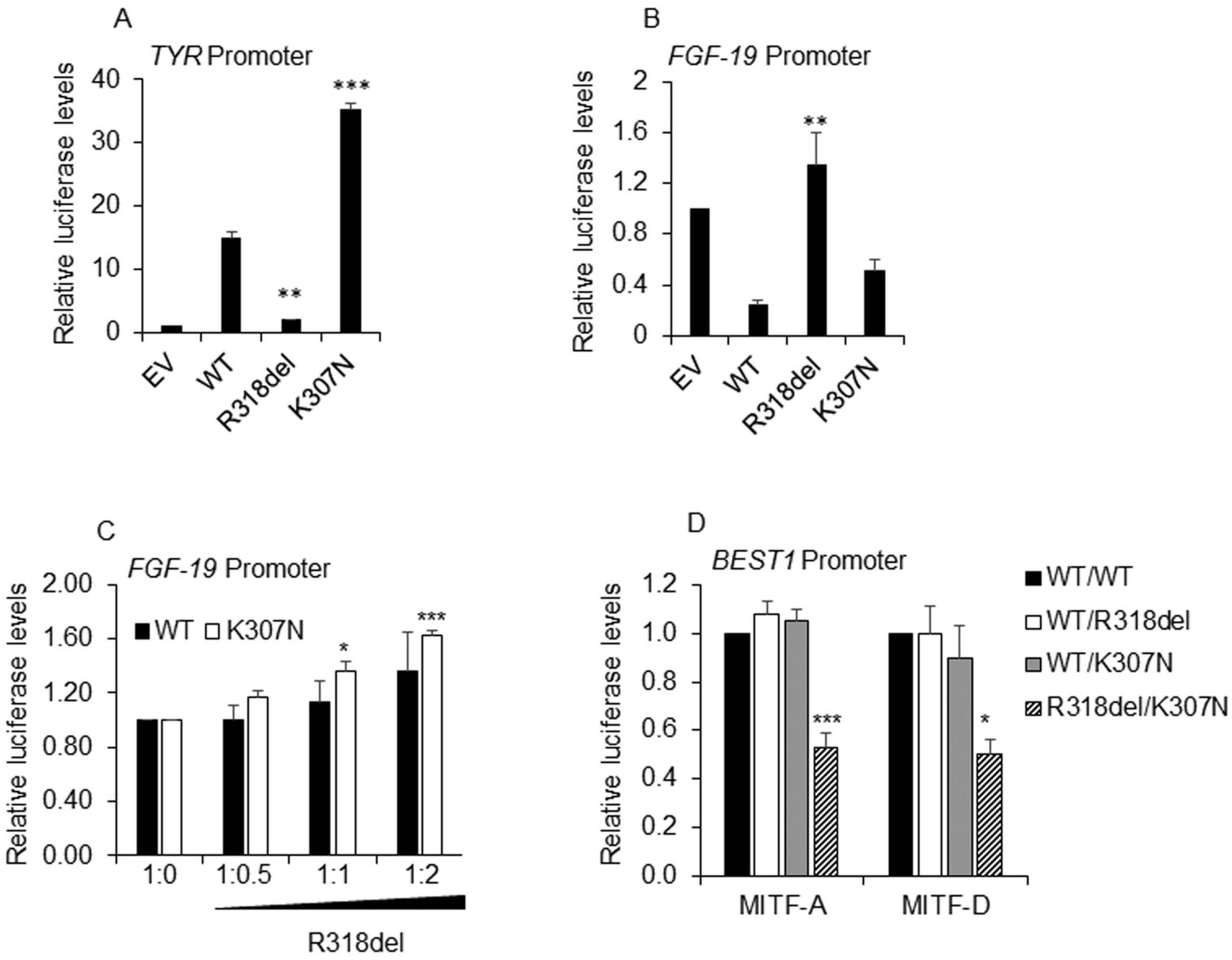
A
TYR Promoter
Relative luciferase levels
40
30
20
10
0
***
**
EV
WT
R318del
K307N
B
FGF-19 Promoter
Relative luciferase levels
2
1.6
1.2
0.8
0.4
0
**
EV
WT
R318del
K307N
C
FGF-19 Promoter
Relative luciferase levels
2.00
1.60
1.20
0.80
0.40
0.00
WT
K307N
*
***
1:0
1:0.5
1:1
1:2
R318del
D
BEST1 Promoter
Relative luciferase levels
1.2
1.0
0.8
0.6
0.4
0.2
0.0
***
*
MITF-A
MITF-D
WT/WT
WT/R318del
WT/K307N
R318del/K307N

Figure S4. Transactivation of MITF-responsive genes by WT and mutant MITF protein.

(A and B) The K307N mutant protein activated the *TYROSINASE* (*TYR)* promoter more than WT MITF and repressed the *FGF-19* promoter. The R318del mutant or empty vector (EV) did not activate nor repressed the studied promoters. (C) Repression of *FGF-19* gene promoter by WT and K307N mutant MITF-A in the presence of R318del mutant. The R318del mutant in increasing concentrations (0, 50, 100 and 200 ng) caused de-repression of FGF-19 promoter by WT-MITF (solid bars, statistically not significant). This is evident by the increase in *FGF-19* promoter trans-activation with increasing concentration of R318del mutant. In contrast, a similar de-repression caused by increasing concentrations of R318del in the presence of K307N was observed to be statistically significant (open bars, $P<0.005$). (D) Transactivation of the RPE specific *Best1* promoter by combination of WT and mutant MITF. Mouse MITF is known to activate the murine *Best1* gene promoter, specific to the retinal pigmented epithelium. A dual luciferase assay was performed to study the effect of the MITF mutation combinations (similar to the genotype of members of family 1) on the activation of this promoter. HEK293 cells were co-transfected with equal amounts of WT and mutant MITF isoforms or the two mutants together with the *Best1* luciferase promoter construct. The promoter activation was observed to be significantly reduced when the two mutants (corresponding to the genotype of proband I) were transfected. Interestingly the relative luciferase levels were similar for the WT/mutant (genotype of affected parents) combinations and WT alone (genotype of unaffected sibling). All comparisons are in reference to the WT-MITF, *P* values were calculated using the two-sided Student's *t* test. *$P<0.05$, **$P<0.01$, ***$P<0.005$.

Table S1: Sequences of the primers and probes used in the study.

Primers/ probes	**Sequence**	
MITF-A	5'-GCGGGAAAGCTTCAGTCCGAATCGGGGATCG-3'	Forward
MITF-D	5'-CCTCCAAGCTTACATCACGCATCTTGCTACG-3'	Forward
MITF-A & D	5'-GGGAGTCTAGACTAACAAGTGTGCTCCGTCTC-3'	Reverse
MITF-A	5'ATGGACTACAAAGACGATGACGACAAGGCGGGAAAG CTTCAGTCCGAATCGGGGATCG-3'	Forward
MITF-D	5'ATGGACTACAAAGACGATGACGACAAGCCTCCAAGCT TACATCACGCATCTTGCTACG -3'	Forward
MITF-A & D	5'-ATAGACCCGGGAGTGTGCTCCGTC-3'	Reverse
M-Box	5'-IR700/GAAAAGTCAGTCATGTGCTTTTCAG-3'	Probe
E-Box	5'- IR700/AAAGAGTAGCACGTGCTACTCAGA-3'	Probe

References

1. Vachtenheim, J. and Drdová, B. *Pigment Cell Res.* **17**, 43-50 (2004).

2. Krieger, E. *et al. Proteins* **47**, 393–402 (2002).